Implementation of a Cognitive Radio Front-End Using Rotatable Controlled Reconfigurable Antennas

Y. Tawk, Student Member, *IEEE*, J. Costantine, Member, *IEEE*, K. Avery, Member, *IEEE,* and C. G. Christodoulou, Fellow Member, *IEEE*

***Abstract*—This paper presents a new antenna system designed for cognitive radio applications. The antenna structure consists of a UWB antenna and a frequency reconfigurable antenna system. The UWB antenna scans the channel to discover "white space" frequency bands while tuning the reconfigurable section to communicate within these bands. The frequency agility is achieved via a rotational motion of the antenna patch. The rotation is controlled by a stepper motor mounted on the back of the antenna structure. The motor's rotational motion is controlled by LABVIEW on a computer connected to the motor through its parallel port. The computer's parallel port is connected to a NPN Darlington array that is used to drive the stepper motor. The antenna has been simulated with the driving motor being taken into consideration. A good agreement is found between the simulated and the measured antenna radiation properties.**

***Index Terms*—cognitive radio, reconfigurable antenna, stepper motor, UWB.**

I. Introduction

A cognitive radio system is able to communicate efficiently across a channel by altering its frequency of operation based on the constant monitoring of the channel spectrum. This system is able to continuously monitor gaps (white spaces) in the finite frequency spectrum occupied by other wireless systems, and then dynamically alter its transmit/receive characteristics to operate within these unused frequency bands; thereby minimizing interference with other wireless systems and maximizing throughput [1]. This capability requires a "sensing antenna" that continuously monitors the wireless channel searching for unused carrier frequencies, and a "reconfigurable transmit/receive antenna"' to perform the data transfer [2]. .

The cognitive radio communication schemes have begun to receive a lot of attention with the advent of 3G and 4G mobile communication standards. Various designs and architectures have emerged. In [3], a quad-antenna with a directional radiation pattern is presented. The operating frequency can be adjusted by the use of MEMS switch making it suitable for cognitive radio applications. A reconfigurable slot antenna for cognitive radio applications is presented in [4]. The antenna can be switched between any one of three discrete states. In [5], it is shown that once a cognitive design manages to learn the RF environment, one can use the collected data to train reconfigurable antennas to adapt to any change in the RF environment. The authors in [6] incorporate both the sensing and the reconfigurable antennas into the same substrate. The reconfigurable antenna is able to tune between 3GHz-5GHz and 5GHz-8GHz. A coupling of less than -10 dB was achieved between the sensing and the reconfigurable antenna. A reconfigurable C-slot microstrip patch antenna is proposed in [7]. Reconfigurability is achieved by switching on and off two patches using PIN diodes. The antenna can operate in a dual-band or in a very wide band mode. In [8], a combination of wideband and narrowband antennas into the same volume is presented. The wideband antenna is a CPW fed printed hour-glass shaped monopole which operates from 3 to 11GHz. The narrowband antenna is a microstrip patch printed on the reverse side of the substrate, and connected to the wideband antenna via a shorting pin and designed to operate from 5.15 to 5.35GHz. Another design was presented in [9] where the antenna reconfiguration was achieved through slot rotation. Each slot rotation redirects the surface current distribution creating an indirect reconfigurable feeding. This antenna achieves a different resonant frequency for each slot position.

In this paper a new reconfigurable antenna design is presented. The antenna structure incorporates both a sensing and a reconfigurable antenna module into the same substrate. The sensing antenna covers the band from 2GHz to 10 GHz, while the reconfigurable antenna is able to tune its operating frequency through the entire band covered by the sensing antenna. Reconfigurability is obtained by feeding at different instances, different antenna patches. This reconfiguration is achieved by a rotational motion. A detailed explanation of the

Y. Tawk and C. G. Christodoulou are with the Department of Electrical and Computer Engineering, University of New Mexico, Albuquerque, NM, USA e-mail: (yatawk, christos@ece.unm.edu)

J. Costantine is with the Electrical Engineering Department, California State University Fullerton, Fullerton, CA email: (joseph.costantine@gmail.com)

K. Avery is with the Air Force Research Laboratory, Space Vehicles Directorate Kirtland AFB, NM , USA email: (keith.avry@kirtland.af.mil)

reconfiguration is discussed in section II. The control mechanism via a stepper motor is shown in Section III and the measurement data are shown in Section IV.

II. Antenna Structure

The antenna is printed on a 70mm x 50mm Rogers Duroid 5880 substrate with a dielectric constant of 2.2 and a height of 1.6 mm. The corresponding antenna structure is shown in Fig.1. The left module is the sensing antenna while the right part is the reconfigurable section.

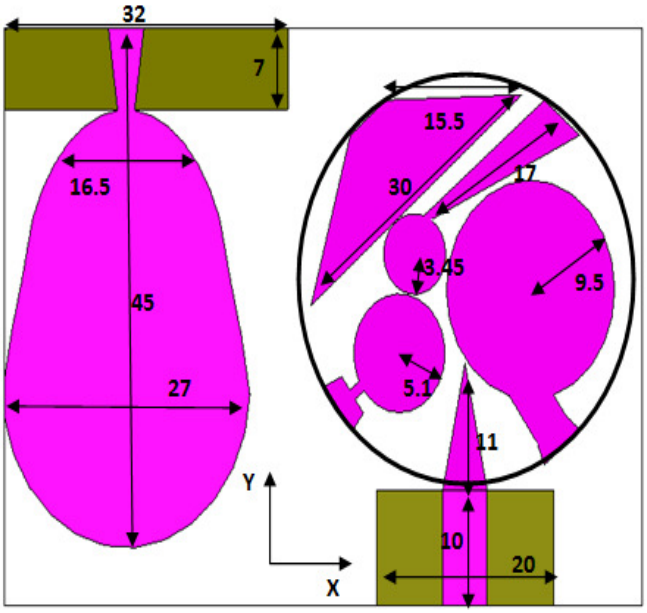

Fig. 1. The antenna structure (dimensions in mm)

A. Sensing Antenna

The sensing antenna is a modified egg-shaped printed monopole antenna. It has a partial ground of dimensions 32mm x 7mm. A tapered stripline is feeding the antenna for better impedance match over the entire bandwidth of interest. This antenna is able to scan the spectrum from 2 to 10 GHz. The computed antenna radiation patterns at f=3 GHz, 6 GHz and 9 GHz in the X-Z plane are shown in Fig.2. The antenna possesses an omni-directional radiation pattern and is able to radiate above and below the substrate due to the fact that it has a partial ground.

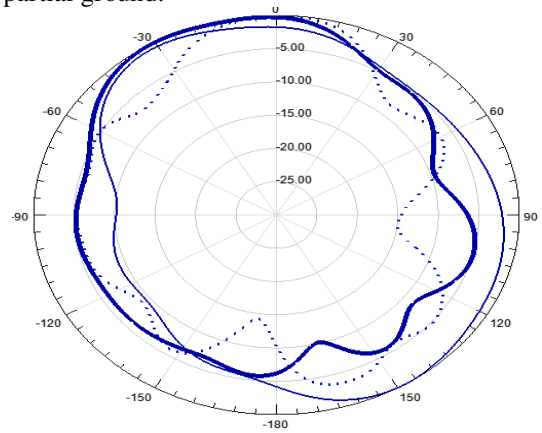

Fig. 2. UWB Antenna Radiation Pattern at f=3 GHz (thin line), 6 GHz (thick line), and 9 GHz (dotted line)

B. Reconfigurable Antenna

Reconfigurable antennas have been implemented so far using RF MEMS [10], PIN diodes [11], or lumped elements [12]. In this work, we propose a new technique which is based on the rotational motion of the antenna structure. The advantage of this technique is that no bias lines are needed for the activation/ deactivation of the switches. In fact the use of bias lines might affects the EM performance of the antenna and adds further complexity to the antenna structure.

In this work, the frequency tuning is achieved by physically altering the patch shape. A circular substrate section holding five different antenna patches is rotated via a stepper motor. A 50 Ω stripline overflows the rotating section in order to guarantee contact between the rotating circular patch and the feeding line. At each rotation stage, the stripline excites a different patch and a different frequency is achieved. The rotation mechanism is described briefly in Fig.3. The stepper motor is modeled in HFSS with the antenna structure to account for its effect. The stepper motor's characteristics are extracted from [13].

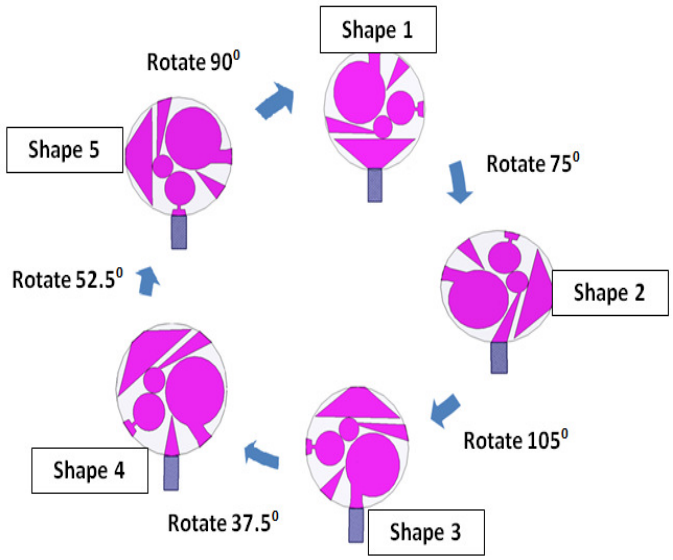

Fig. 3. Antenna reconfigurability process

III. Stepper Motor Controller

The stepper motor used in this work rotates in 7.5 degree steps, and for each step 2 coils should be activated simultaneously [13]. The sequences of coil activation are summarized in Table I, where "1/0" denotes whether the corresponding coil is "activated / deactivated". The amount of steps needed to go from one shape to another is summarized in Fig.4. The stepper motor is attached to the back of the rotatable circular patch. Two plastic screws are used to hold the stepper motor to the antenna substrate as shown in Fig.5. The motor rotating part consists of a metallic cylinder of length 1 cm and diameter 1 cm. This part is soldered to the back of the rotating circular patch in order to achieve the required rotation.

The stepper motor is connected to a computer via a parallel

port and the control of the motor is achieved by using LABVIEW. A LABVIEW code was implemented to send to the pins of the parallel port (pin 2 till 5) one of the four sequences shown in Table I.

TABLE I
COIL ACTIVATION SEQUENCE

	Coil 1	*Coil 2*	*Coil 3*	*Coil 4*
Sequence 1	1	0	1	0
Sequence 2	1	0	0	1
Sequence 3	0	1	0	1
Sequence 4	0	1	1	0

Each of the four outputs from the parallel port (0V/5V TTL signal) is connected to a high voltage, high current Darlington array. The Darlington array, considered as the driver of the stepper motor, consists of two pairs of transistors for higher gain. Each output from the Darlington array is connected to one of the four coils of the stepper motor. In this work, the ULN2003 seven open collector Darlington pairs is used [14]. A 12 V power supply is needed for the stepper motor and the ULN2003. A flowchart of the LABVIEW code is shown in Fig.6.

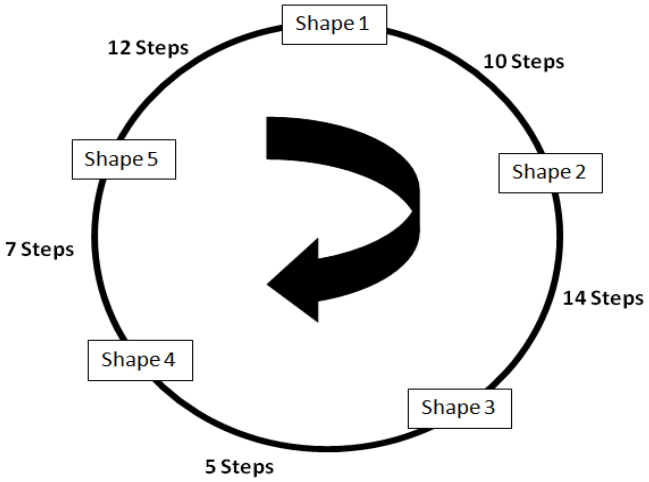

Fig. 4. The number of steps needed for each rotation

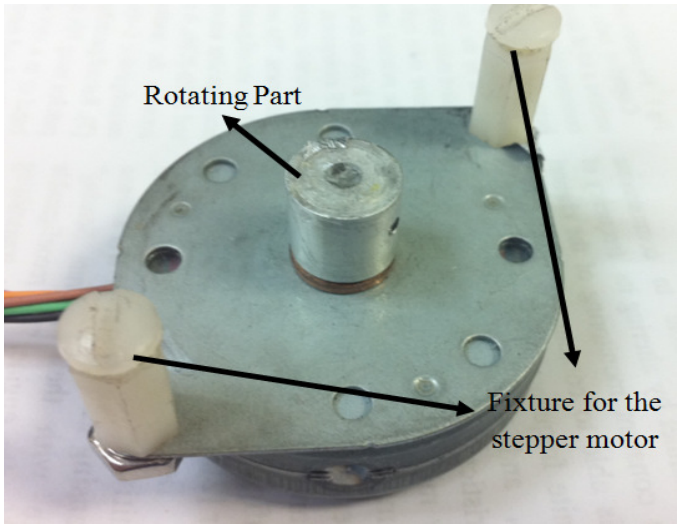

Fig. 5. The stepper motor used in this work

IV. FABRICATION AND RESULTS

A prototype antenna is fabricated and tested. The stepper motor incorporated in the back of the reconfigurable rotating antenna section is connected to the controlling circuit as discussed in the previous section. The fabricated antenna is shown in Fig.7.

A. Sensing Antenna Results

As shown in Fig.1, the sensing antenna has a total length of 38mm ≈ 0.25×λ (where λ corresponds to the lowest frequency at '2 GHz'). The comparison between the simulated and the measured return loss for the sensing antenna is shown in Fig. 8. This comparison corresponds to the case when the reconfigurable section is at the initial position shown in Fig.7. It is noted that the UWB performance of the antenna remains constant for all the reconfigurable section positions.

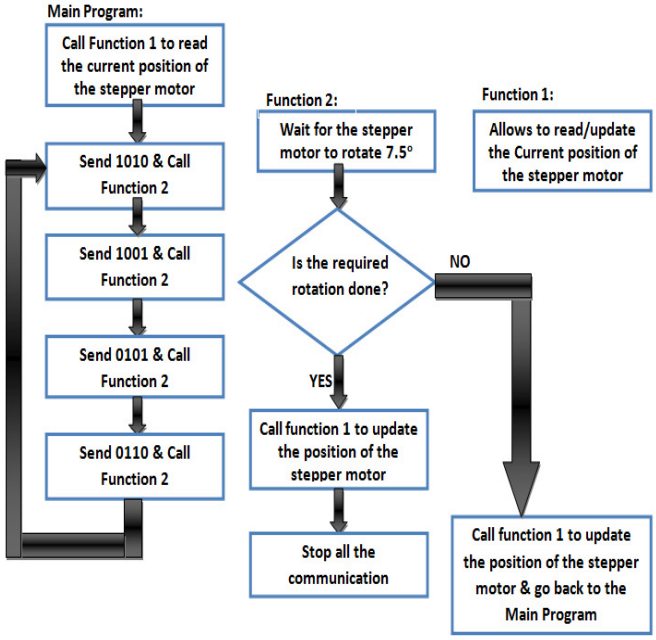

Fig. 6. The flowchart of the LABVIEW algorithm

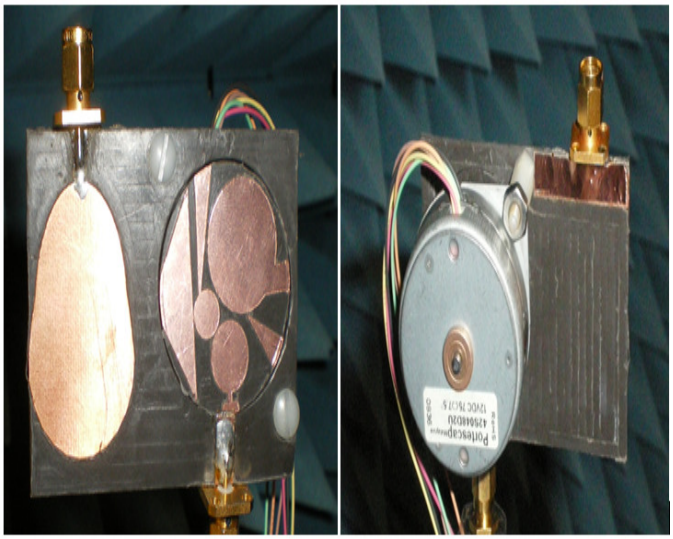

Fig. 7. The Fabricated antenna

B. Reconfigurable Section Results

The reconfigurable section consists of a rotating 18 mm radius circular substrate section that carries five different patches. Each patch on the rotating section resonates at a different band from 2GHz up to 10 GHz. The five different patches cover collectively the whole band (2- 10 GHz). The dimensions and the position of the different shapes were optimized using HFSS. All the shapes are fed via a 10mm × 5mm feeding line and they share a 20 mm × 10mm partial ground. The covered band for each shape is summarized in Table II.

To ensure a good connection between the rotating circular patch and the feed line, a 50 Ω stripline overflows the rotating circular section. It is soldered to the feed line; a zoomed view of the connection between the feed line and the rotating circular part is shown in Fig.9.

The comparison between the simulated and the measured return loss for the rotating section is shown in Fig.10. Each band is labeled by the corresponding antenna shape number. An agreement is noticed between both data.

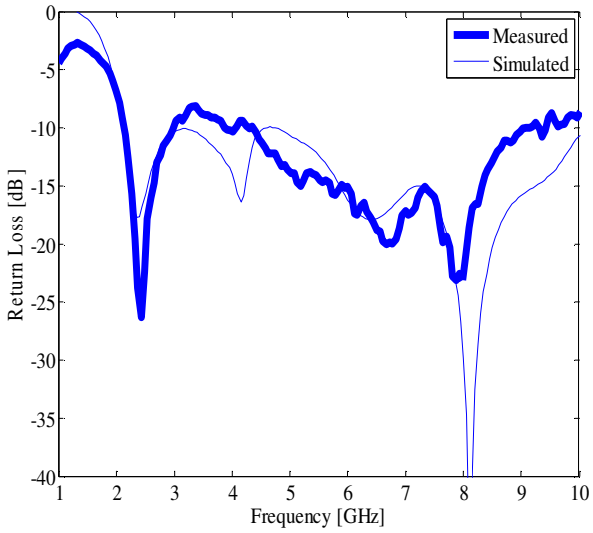

Fig. 8. The sensing antenna return loss

TABLE II
Frequency Reconfigurability

	Covered Band [GHz]
Shape 1	3.4-5.56
Shape 2	6.3-10
Shape 3	2.1-3
Shape 4	5.4-6.2
Shape 5	3-3.4

TABLE III
Measured Coupling

	Min/Max[dB]
Shape 1	-45/-25
Shape 2	-32/-23
Shape 3	-30/-20
Shape 4	-28/-25

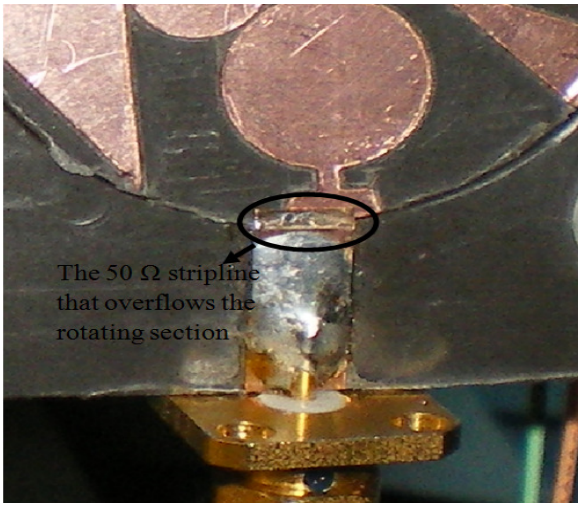

Fig. 9. A zoomed view of the connection between the feed line and the rotating part

C. Coupling between the two antenna sections

For any cognitive radio application the sensing and the reconfigurable antennas must be isolated. In order to quantify the amount of mutual-coupling induced between the two antenna sections, we should look at the transmission between the two antenna ports. The comparison between the simulated and the measured coupling ($|S21|^2$) is shown in Fig.11. This plot corresponds to the case when the reconfigurable antenna is at the position shown in Fig.7. A coupling of less than -20 dB is obtained due to the fact that the two antenna structures are fed from the opposite edges of the substrate. The min/max values of the measured coupling for the other positions of the reconfigurable antenna are summarized in Table III. These values correspond to the frequency band where each shape of the reconfigurable antenna operates as summarized in Table II.

D. Radiation Pattern of the Reconfigurable Antenna

The comparison between the simulated (thick line) and the measured (thin line) radiation pattern for the reconfigurable antenna section in the X-Z plane is shown in Fig.12 for different frequencies. A good agreement is noticed and the antenna preserves its omni-directional radiation pattern for all the different stages of the rotating section making it very convenient for cognitive radio applications. It is noticed that the stepper motor adds constructively to the antenna radiation pattern.

The peak antenna gain values for the 5 different patches of the rotating section, at the same frequencies used in the radiation pattern measurement shown in Fig. 12, are summarized in Table IV.

TABLE IV
Antenna Peak Gain

	Gain [dB]
Shape 1	6.62
Shape 2	8.45

Shape 3	7.77
Shape 4	6.67
Shape 5	7.4

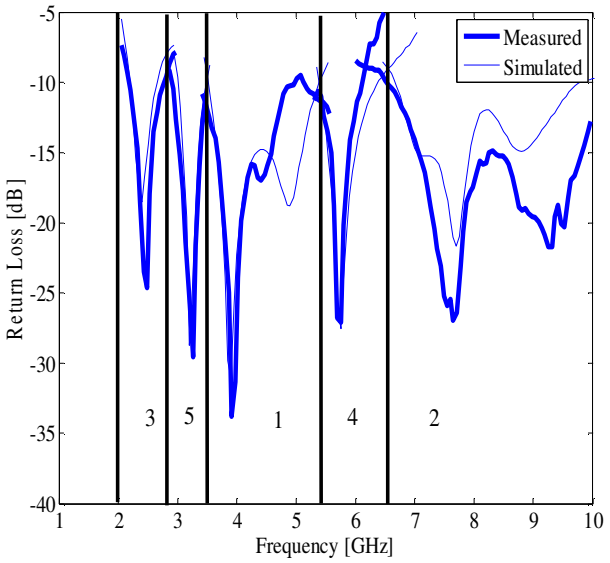

Fig. 10. A comparison between the measured and simulated return loss for the reconfigurable antenna section

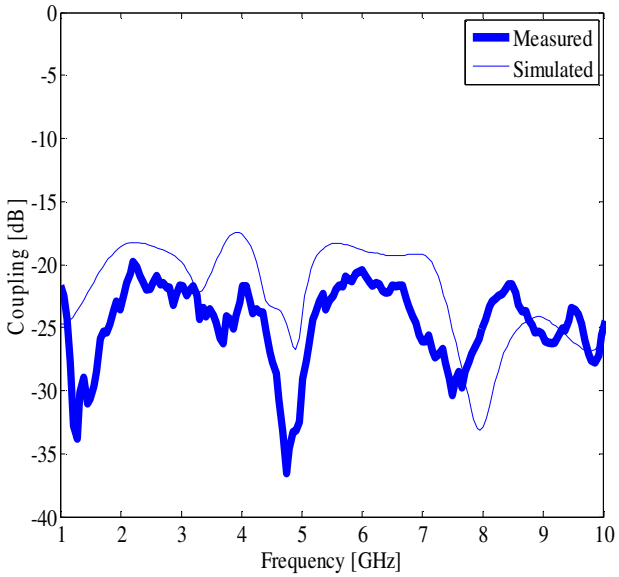

Fig. 11. The coupling between the two sections

V. Conclusion

This paper presents an antenna design suitable for cognitive radio applications. The antenna is composed of a sensing section, achieved by an UWB printed monopole antenna and a reconfigurable section, represented by a rotating circular substrate section carrying five different patches. Each patch operates at a different frequency band when fed by a stripline that excites each particular shape upon rotation. The antenna system is fabricated and measured. A stepper motor controlled by LABVIEW through a computer's parallel port rotates the circular section carrying the different patches. The comparison between the measured and the simulated data is satisfactory. To our knowledge, this is the first antenna designed for cognitive radio that is able to tune throughout the whole band covered by the sensing antenna (2GHz-10GHz).

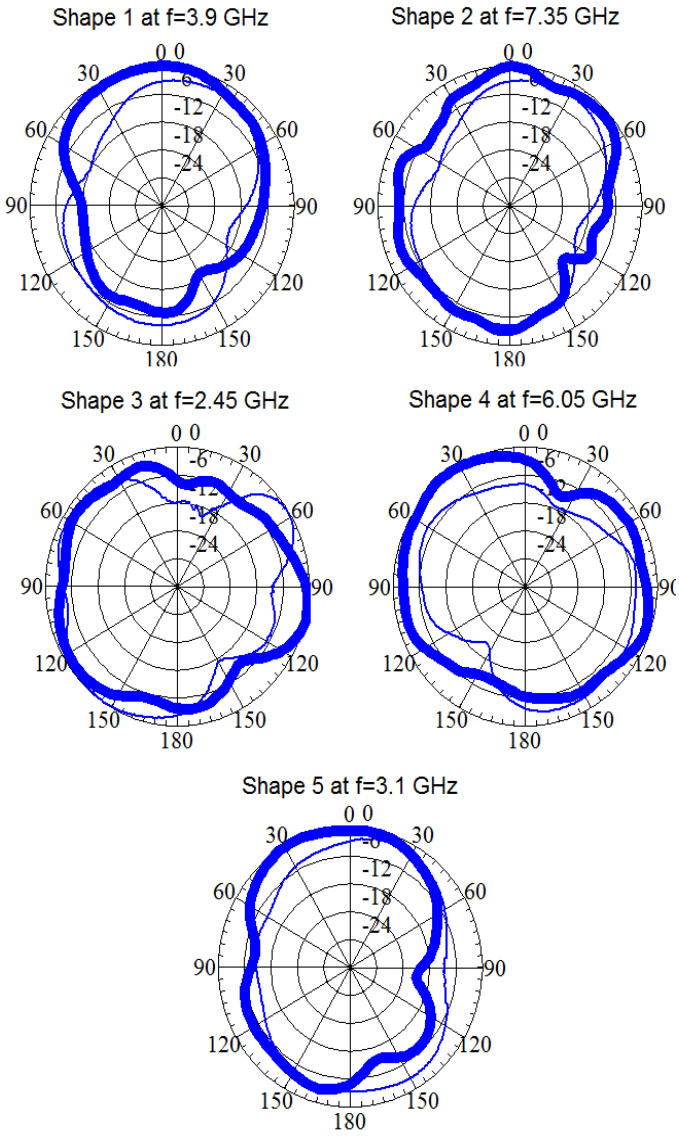

Fig. 12. The simulated (thick line) and the measured (thin line) radiation pattern for the reconfigurable antenna

Acknowledgment

This work was supported by the Air Force Research Lab/RVSE under contract no. FA9453-09-C-0309.

References

[1] J. Mitola, "Cognitive Radio: An integrated agent architecture for software defined radio", Ph.D. dissertation, Royal Institute of Technology (KTH), Stockholm, Sweden, 2000

[2] C. G. Christodoulou, "Cognitive Radio: The New Frontier for Antenna Design?", *IEEE Antennas and Propagation Society Feature Article,* www.ieeeaps.org.

[3] G T. Wu, R. L. Li, S. Y. Eom, S. S. Myoung, K. Lim, J. Laskar, S. I. Jeon, and M. M. Tentzeris, "Switchable quad-band antennas for cognitive radio base station applications", *IEEE Transactions on Antennas and Propagation,* vol. 58, n0. 5, pp. 14668-1476, 2010.

[4] J. R. Kelly and P. S. Hall, "Reconfigurable slot antenna for cognitive radio application," *in IEEE Antennas and Propagation Society International Symposium,* 2009, pp. 1-4.
[5] C. G. Christodoulou, "Reconfigurable antennas in cognitive radio that can think for themselves," *in 3rd IEEE International Symposium in Microwave, Antenna, Propagation and EMC Technologies for Wireless Communications,* 2009, pp. K1-K3.
[6] Y. Tawk and C. G. Christodoulou, "A new reconfigurable antenna design for cognitive radio," *IEEE Antennas and Wireless Propagation Letters,* vol. 8, pp. 1378-1381, 2009.
[7] H. F. AbuTarboush, S. Khan, R. Nilavalan, H. S. Al-Raweshidy, and D. Budimir, "Reconfigurable wideband patch antenna for cognitive radio," *in 2009 Loughborough Antennas and Propagation Conference,* 2009, pp. 141-144.
[8] E. Ebrahimi and P. S. Hall, "A dual port wide-narrowband antenna for cognitive radio," *in The Third European Conference on Antennas and Propagation*, 2009, pp. 809–812.
[9] J. Costantine, S. al-Saffar, C. G. Christodoulou, K. Y. Kabalan, A. El-Hajj " The Analysis of a Reconfiguring Antenna With a Rotating Feed Using Graph Models", *IEEE Antennas and Wireless Propagation Letters*, vol.8, pp. 943-946, 2009.
[10] D. E. Anagnostou, G. Zheng, M. T. Chryssomallis, J. C. Lyke, G. E. Ponchak, J. Papapolymerou and C. G. Christodoulou, "Design, fabrication, and measurement of an RFMEMS-based self-similar reconfigurable antenna," *IEEE Transactions on Antennas and Propagation,* vol. 54, no. 2, pp 422-432, Feb. 2006.
[11] M. I. Lai, T. Y. Wu, J. C. Hsieh, C. H. Wang, S. K. Jeng, "Design of reconfigurable antennas based on an L-shaped slot and PIN diodes for compact wireless devices," *IET Microwaves, Antennas & Propagation*, vol. 3, pp. 47-54, 2009.
[12] N. Behdad and K. Sarabandi, "Dual-band reconfigurable antenna with a very wide tunability range", *IEEE Transactions on Antennas and Propagation,* vol. 54, no. 2, pp. 409-416, Feb. 2006.
[13] http://www.digikey.com
[14] http://www.datasheetcatalog.com/datasheets_pdf/U/L/N/2/ULN2003A.shtml